

Spin and orbital magnetism in Fe-Co and Co-Ni alloys

Per Söderlind

Department of Physics, University of Uppsala, Box 530, Uppsala, Sweden

Olle Eriksson

Center for Materials Science and Theoretical Division, Los Alamos National Laboratory, Los Alamos, New Mexico 87545

Börje Johansson

Department of Physics, University of Uppsala, Box 530, Uppsala, Sweden

R. C. Albers and A. M. Boring

Center for Materials Science and Theoretical Division, Los Alamos National Laboratory, Los Alamos, New Mexico 87545

(Received 17 December 1990; revised manuscript received 9 December 1991)

Using the linear muffin-tin orbital method and the virtual-crystal approximation, we have calculated from first principles the spin and orbital moments of Fe-Co and Co-Ni alloys. The spin-orbit interaction was included at the variational step. The calculations also incorporated orbital polarization, which improved the agreement with the experimental orbital moments. While the spin moments were fairly insensitive to the level of approximation and followed the Slater-Pauling curve, the orbital moments exhibited a more complex behavior, where, for example, the crystal structure plays a most decisive role. Finally, enhanced orbital moments are predicted for $\text{Co}_{1-x}\text{Ni}_x$ alloys with $x \sim 0.25-0.5$ in a hypothetical bcc structure, and for $\text{Fe}_{1-x}\text{Co}_x$ alloys with $x \sim 0.25$ in a hypothetical fcc structure.

I. INTRODUCTION

The magnetic properties of the pure elements and the alloys of Fe, Co, and Ni have been extensively studied, both theoretically and experimentally (see, for example, Refs. 1-4). Fe, Co, and Ni have the nice property that they mix with each other and form alloys over the entire concentration range (0-100% alloying), even though each of the pure elements forms in a different crystal structure: Fe (bcc), Co (hcp), and Ni (fcc). The Fe-Co alloys form in the bcc crystal structure for a Co concentration range of 0-80%, and the Co-Ni alloys form in the fcc crystal structure for a Ni concentration range of 10-100%. The complete solubility occurs because the electronic structure and the atomic volumes are so similar. For example, the experimental Wigner-Seitz radii S , which are a measure of the atomic volumes per atom [$(4\pi/3)S^3$ is the atomic volume], are given by⁵ $S(\text{Fe})=2.662$ a.u., $S(\text{Co})=2.621$ a.u., and $S(\text{Ni})=2.602$ a.u.. The difference in electronic structure results because each succeeding element adds one d electron per atom. Because the bands are nearly identical, the main effect is to change the Fermi energy. Thus with these alloys one can hope to study the magnetic properties as a function of the d -band filling.

On the theoretical side, local spin-density approximation (LSDA) calculations for the spin moments have been in good agreement with experiment and to a large extent have explained the magnetic moments for the pure metals.¹⁻³ This is because the LSDA works well for systems such as these where the spin contribution dominates the total magnetic moment (in these systems the orbital mo-

ment is essentially quenched, see below). In order to calculate orbital moments one needs to include the relativistic spin-orbit interaction, which induces an orbital moment; this can be accomplished either by solving the spin-polarized Dirac equation⁶ or by adding the spin-orbit-coupling term to the band Hamiltonian⁷ and treating the spin-orbit effect self-consistently at each variational step. This accounts for the interactions giving rise to Hund's first and third rules for atoms. Furthermore, a good calculation of the orbital contribution to the total moment also requires including interactions responsible for Hund's second rule, namely, that for the atom the total orbital moment should be maximized for a maximum spin configuration. We have earlier suggested corrections to the LSDA that take into account interactions responsible for all three of Hund's rules.⁸ Recently this formalism has been used successfully to calculate the orbital magnetism for pure Fe, Co, and Ni.⁹

In this study we attempt to calculate and explain the magnetic spin and orbital moments of the Fe-Co and Co-Ni alloys; we will compare our results to the experimental data recently reviewed in Ref. 10. For these alloy calculations we have adopted the simplest possible approximation, namely, the virtual-crystal approximation (VCA), in which the atoms in the true alloy are replaced by "average" atoms, whose atomic number is the concentration-weighted atomic number of the alloy. Thus, for an alloy with equal amounts of, for instance, iron and cobalt, we replace the nuclear charge (Z) and the number of valence electrons (n_{val}) with the alloy average, i.e., $Z=26.5$ and $n_{\text{val}}=8.5$. Although there certainly exist better schemes for calculating the electronic structure of alloys (for in-

stance, the coherent potential approximation¹¹), it has been shown that the VCA yields integrated properties (for instance, magnetic moments) in fair agreement with experiment.¹² Generally, it can be said that the VCA is a good approximation for systems where the energy bands are more or less rigid when the alloy concentration changes. Furthermore, the chosen approach has the advantage, in addition to its simplicity, of neglecting both off-diagonal as well as diagonal disorder,¹³ and hence brings out the pure band-filling effects on the magnetic moments. In order to disentangle band-filling effects from changes in the crystal structure, we have also performed calculations in both the bcc and the fcc phases for all alloy concentrations, and have made calculations for the FeCo and CoNi ordered alloys in the CsCl structure.

II. DETAILS OF CALCULATIONS

The electronic structure was calculated with the linear muffin-tin orbital (LMTO) method; the combined correction terms and the spin-orbit coupling at each variational step⁷ were included. We used s , p , and d partial waves for the results presented here, however, we tested the importance of including f partial waves for some alloys and the resulting spin and orbital moments were within a few percent of the s , p , and d calculation. The von Barth-Hedin¹⁴ LSDA potential was used. In addition, we included orbital polarization in the same way as described previously,⁸ namely, the orbitals with the spin, orbital, and magnetic quantum numbers (σ, l, m_l) were shifted by an amount $BL_\sigma m_l$. Here L_σ is the total orbital moment of the states with spin σ , and B is the Racah parameter¹⁵ for the d electrons. B was recalculated at each iteration as a linear combination of Slater integrals involving radial wave functions which were calculated for a fixed energy at the center of the occupied part of the energy band (calculating B at different energies gave only a small variation). The total orbital moment is calculated as the sum of the two spin components, i.e., $L = \sum_\sigma L_\sigma$. The calculations were performed at various levels of approximation: standard spin-polarized calculations (SP), spin-polarized calculations with the spin-orbit coupling included at each variational step (SO), and calculations including all of the above effects (OP, spin polarization, spin-orbit coupling, and orbital polarization). The number of \mathbf{k} points of the irreducible wedge of the Brillouin zone was increased until the results were converged to within a few percent. The Bravais lattice of a ferromagnetically ordered metal has the same shape of the Brillouin zone (BZ) as it has in the paramagnetic phase since the spin on each atom site is parallel and the primitive translation vectors will not be affected by this. But in the presence of a magnetization vector \mathbf{M} that couples to the lattice there may be a reduction of symmetry of the Bravais lattice, depending on the direction of \mathbf{M} , which then results in an increased irreducible part of the Brillouin zone (IBZ), compared to the paramagnetic case. In our ferromagnetic calculations the magnetization on each site is aligned parallel to the z axis. The cubic symmetries of the bcc, fcc, and simple cubic (sc) crystal structures becomes tetragonal in this case and the IBZ increases from

$\frac{1}{48}$ to $\frac{1}{16}$ of the BZ. There will, however, not be any reduction of the hexagonal symmetry for our choice of magnetization direction and no larger IBZ than $\frac{1}{24}$ of the BZ is needed. This lowering of the cubic symmetry, which was not considered in Ref. 9, has been shown to be important for the accuracy of the orbital moment. The IBZ was sampled at 324 \mathbf{k} points for the hexagonal structure and 405 \mathbf{k} points were used for the cubic structures. Finally, Vegard's law was used to determine the lattice constants for the alloys; when the pure elements did not form in the required structure, the lattice constants were adjusted so as to give the correct volume per atom for the pure elements.

III. RESULTS

The main results of the present investigation are displayed in Fig. 1, where our calculated values are compared with the experimental spin and orbital moments. Our most elaborate calculations (OP) reproduce the experiments quite well for all alloy concentrations. The spin moments are found to follow a Slater-Pauling curve, which relates the spin moment to the filling of the d band. The maximum moment occurs for about 25% Co in Fe; at this concentration the spin-up band is essentially filled. As additional valence electrons are added (by changing the Co and Ni concentrations), the spin-down band be-

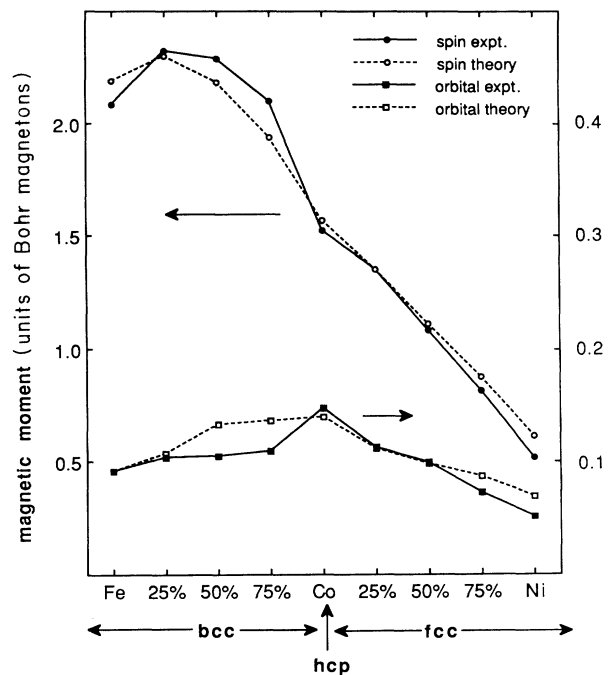


FIG. 1. Calculated and experimental data of the spin and orbital moments for the Fe-Co and Co-Ni alloys. The spin moments are marked by filled (open) circles for the experimental (theoretical) data. The orbital moments are marked by filled (open) squares for the experimental (theoretical) data. The Fe-Co data are for a bcc structure, the Co data are for the hcp structure, and the Co-Ni data are for the fcc structure. The scale for the spin data is to the left and the scale for the orbital data is to the right.

comes more populated, and the spin moment drops accordingly.

The orbital moment (its contribution is between ~4% and ~13% of the total moment) is appreciably smaller than the spin moment and has a quite different concentration dependence. Its calculated values are more sensitive to the level of approximation than the spin moments. This is shown in Fig. 2, where we compare the effects of the (SO) and the (OP) approximations on the orbital moment. Both calculations shown the same trends, but the OP orbital moments, which are in better agreement with experiment, are about 50% larger than those for the (SO). For both cases and for experiment the orbital moment increases with alloy concentration between Fe and Co to a maximum for pure Co, and then decreases continuously for the Co-Ni alloys with an increasing concentration of Ni. The increase of the orbital moment between Fe and Co is surprising, since it is opposite to the decreasing spin moment in this region (and the crystal structure is the same, except for pure Co). However, as we have noticed in a previous paper,⁹ the orbital moments are governed by the spin moment, the crystal structure, and the band filling. Since the crystal structure is the same, and since the spin moment decreases, band-filling effects must be responsible for the increasing orbital moment.

To investigate the effects of crystal structure we have also calculated the spin and orbital moments for all (Fe-Co-Ni) alloy concentrations in both the fcc and bcc phases (see Fig. 3). Although the difference in spin mo-

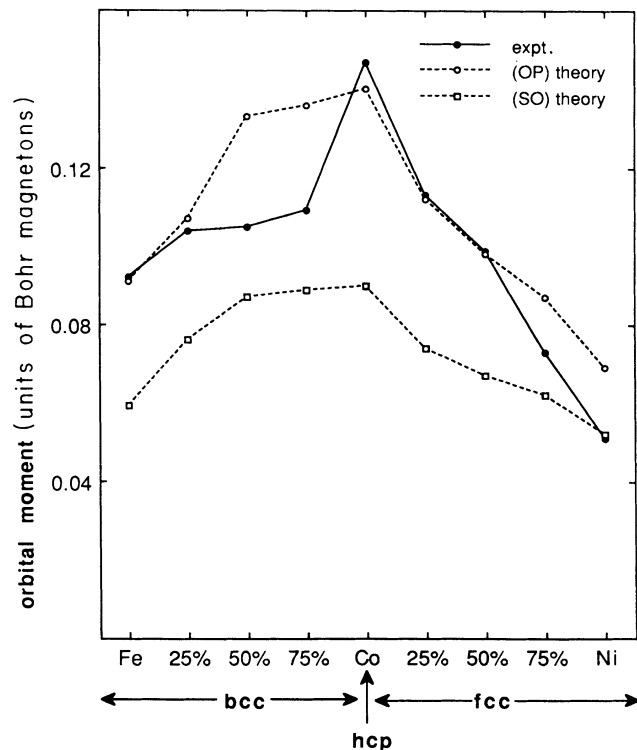


FIG. 2. Calculated (SO), (OP), and experimental data for the orbital moments for the Fe-Co and Co-Ni alloys. The Fe-Co data are for the bcc structure, the Co data are for the hcp structure and the Co-Ni data are for the fcc structure.

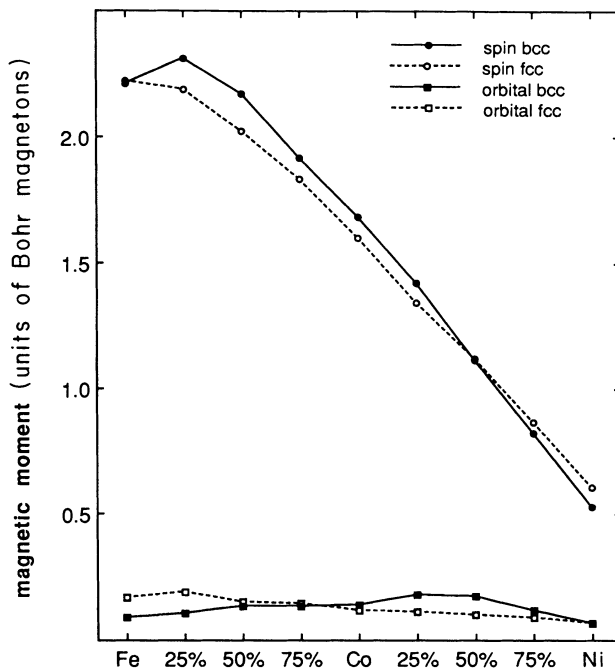


FIG. 3. Calculated spin and orbital moments for the Fe-Co and Co-Ni alloys in the fcc (open) and bcc (filled) phase.

ment between the two structures is very small, in the bcc structure the spin moment reaches a maximum at a concentration of 25% Co in Fe, whereas in the fcc phase the spin moment drops monotonically from Fe to Ni. This suggests that the Fe spin-up band is not quite filled in the bcc phase,¹⁶ whereas it is essentially filled for the fcc

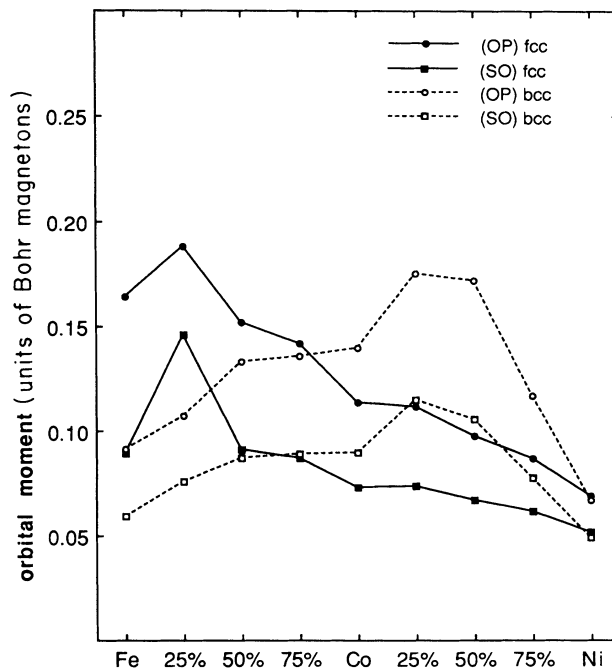


FIG. 4. Calculated (SO), (OP) orbital moments for the Fe-Co and Co-Ni alloys in the fcc and bcc phases.

phase. Here, we note that the $2.2\mu_B$ spin state in fcc Fe is a metamagnetic state,¹⁷ which was calculated with the fixed-spin-moment (FSM) method.¹⁸ However, only a slight expansion of the volume is required to stabilize this spin state; this causes only a small change in the spin moment.

The orbital moments show a more complex difference between the two phases. The fcc orbital moments have a maximum for 25% Co in Fe, followed by a decrease for the rest of the series, whereas the bcc structures show an increase until reaching a maximum for the 25–50% Co–Ni alloy. To present this effect more clearly we show in Fig. 4 the orbital moments from the (SO) and (OP) calculations. To illustrate this even further we show in Fig. 5 the orbital moments [obtained from (OP) calculations] decomposed into spin-up and spin-down contributions. The spin-up contribution is more or less featureless and very small, since the spin-up band is almost filled. Therefore in the following analysis we will neglect this contribution completely. Except for the early maximum at $\text{Fe}_{0.75}\text{Co}_{0.25}$ the spin-down orbital contribution for the fcc structure is decreasing smoothly across the series just as does the total spin moment plotted in Fig. 3, and the orbital and spin moments therefore show a clear correlation. This should intuitively be the case since the orbital moment from the (SO) calculation arises from the spin-orbit coupling only, and the (OP) results generally seem to enhance the (SO) results with about 50%. The expected increase of the orbital moment with increasing spin moment is worth a comment. Even if the spin-orbit coupling is accounted for, there will not be an orbital moment, unless there is a spin moment. For a given eigen-

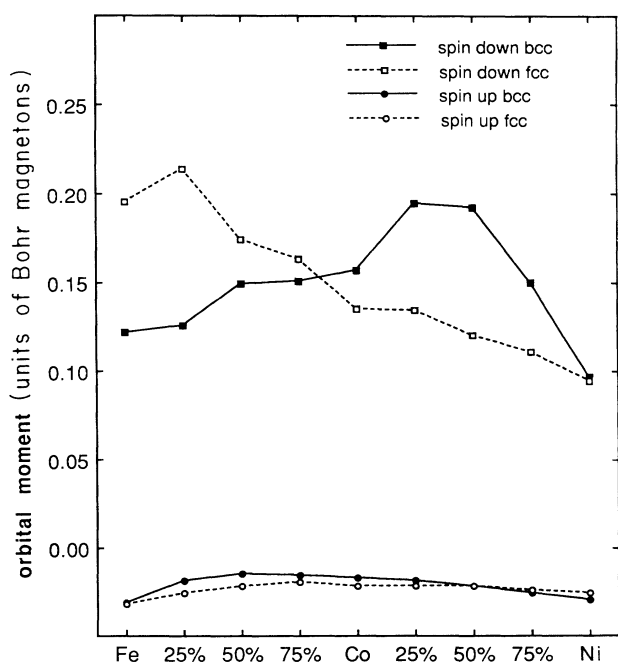


FIG. 5. Calculated (OP) orbital moments, decomposed into the different spin contributions, for the Fe-Co and Co-Ni alloys in the fcc and bcc phase.

value there will not be an equal amount of $+m_l$ and $-m_l$ character of spin σ , and one would therefore expect an orbital moment. However, if there is not spin splitting, the orbital moment of spin band σ will be canceled by the orbital moment of spin band $-\sigma$, and the net orbital moment is equal to zero. However, if a spin moment is present, the spin degeneracy is lifted and a net orbital moment develops. For larger spin splittings (larger spin moments) one would intuitively expect a larger orbital moment. The results for the bcc structure are in sharp contrast to these ideas, however, since we find that the orbital moment increases monotonically (although the spin moment decreases monotonically) until it reaches a maximum for the 25% Co–Ni alloy. From Fig. 5 it is seen that the explanation for the peculiar behavior of the total orbital moment lies in the spin-down contribution.

Using simple model calculations it has been argued that the orbital moment should be enhanced when the

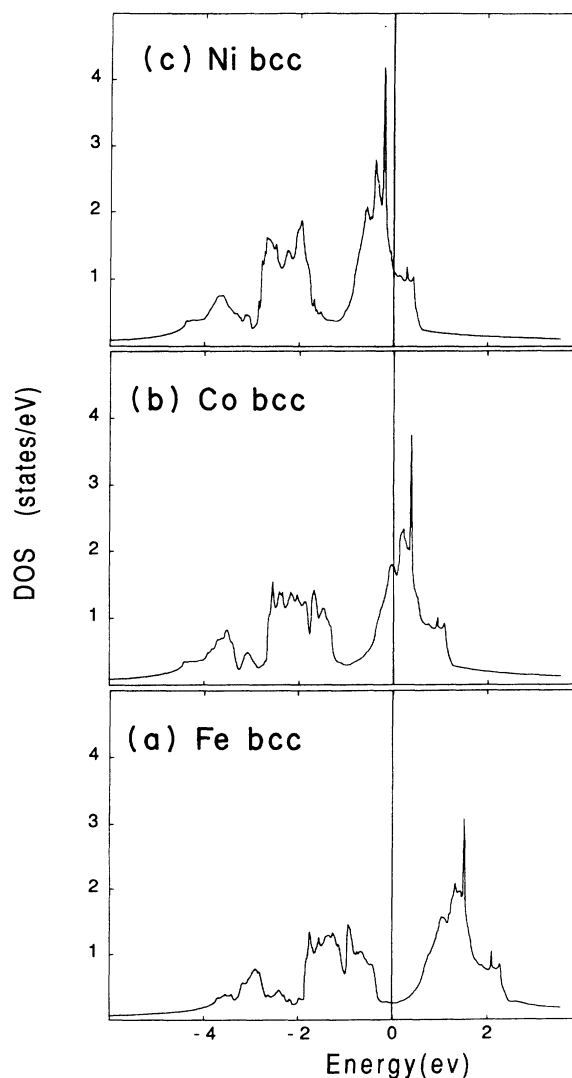


FIG. 6. Calculated spin-down d DOS for (a) Fe, (b) Co, and (c) Ni in the bcc phase. Energies are in eV, and E_F is at zero energy.

density of states (DOS) at E_F is high.^{9,19} To investigate this correlation we show the calculated spin-down DOS of Fe, Co, and Ni in Fig. 6 for the (SO) approximation. Notice that the DOS's of the three systems look very similar, and that the main effect of the progressive filling of the $3d$ band is to move E_F to higher energies. Moreover, we see that for $\sim 50\%$ Co-Ni alloys the Fermi level cuts the DOS at a very high peak, and the correlation between enhanced orbital moments (which reaches a maximum at these concentration) and a high DOS at E_F (Refs. 9 and 19) holds for these systems as well.

As seen from Fig. 6 the DOS's for Fe, Co, and Ni can to a good approximation be considered as rigid. For this reason we introduce the orbital number of states, $P(E)$, and the orbital density of states, $O(E)$,

$$O_{m_l}^\sigma(E) = m_l D_{m_l}^\sigma(E) - m_l D_{-m_l}^\sigma(E), \quad (1)$$

$$P_{m_l}^\sigma(E) = \int_{-\infty}^E O_{m_l}^\sigma(E') dE', \quad (2)$$

where the orbital moment is the sum of the various m_l and spin components, $L = \sum_{m_l, \sigma} P_{m_l}^\sigma(E_F)$ (E_F is the Fermi energy). Using the rigid band approximation one can calculate the orbital moment for any alloy by means of these equations. We have performed an (OP) calculation of the orbital density of states and orbital number of

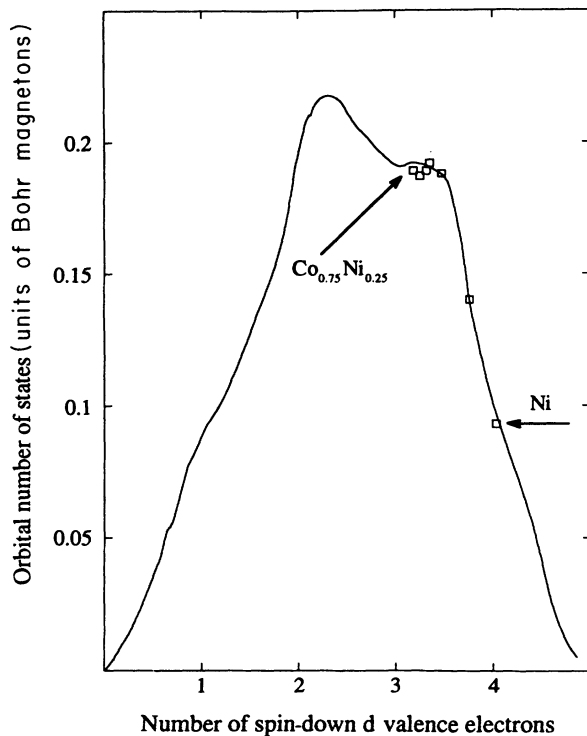


FIG. 7. Calculated (OP) spin-down contribution to the orbital number of states for the d electrons. Open squares refer to the corresponding self-consistently calculated orbital moment of the alloys $\text{Co}_{0.75}\text{Ni}_{0.25}$, $\text{Co}_{0.70}\text{Ni}_{0.30}$, $\text{Co}_{0.65}\text{Ni}_{0.35}$, $\text{Co}_{0.60}\text{Ni}_{0.40}$, $\text{Co}_{0.50}\text{Ni}_{0.50}$, $\text{Co}_{0.25}\text{Ni}_{0.75}$, and Ni.

states for the bcc $\text{Co}_{0.5}\text{Ni}_{0.5}$ alloy, used the rigid band approximation, and computed the orbital moments from Eq. (2) (Fig. 7). Since the spin-down d contribution to the orbital number of states dominates, we show only this component in Fig. 7. To investigate the validity of using this approximation we performed additional bcc (OP) calculations for the alloys $\text{Co}_{0.7}\text{Ni}_{0.3}$, $\text{Co}_{0.65}\text{Ni}_{0.35}$, and $\text{Co}_{0.6}\text{Ni}_{0.4}$. We then plotted the spin-down d contribution to the orbital moment (OP calculation) for the bcc alloys $\text{Co}_{0.75}\text{Ni}_{0.25}$, $\text{Co}_{0.70}\text{Ni}_{0.30}$, $\text{Co}_{0.65}\text{Ni}_{0.35}$, $\text{Co}_{0.60}\text{Ni}_{0.40}$, $\text{Co}_{0.50}\text{Ni}_{0.50}$, $\text{Co}_{0.25}\text{Ni}_{0.75}$, and Ni in Fig. 7 (open squares). Notice from Fig. 7 that the self-consistently calculated spin-down d contributions to the orbital moment are quite close to the results expected by using Eq. (2), together with rigid bands. From this it seems that band filling is important in determining the orbital contribution to the moment. In connection to this it is interesting to observe that for the alloys with Co concentration between 75% and 50%, E_F lies in a high peak in the spin-down DOS (the spin-up DOS is essentially filled and will not play a role). Therefore, when changing the alloy concentration (in the rigid band approximation this simply means shifting E_F so that the right number of valence electrons is obtained), a smaller shift of the (rigid) bands is obtained, compared to the case when the DOS around E_F is low. If band filling is important for determining the orbital moments one would expect the change in orbital moments to be larger when the shifts of the bands are large, and correspondingly smaller when the shifts are small. For the alloys with Co concentrations between 75% and 50% the shifts are indeed small (since E_F lies in a high peak of the spin-down DOS) and the change in orbital moments also small (the orbital moment is almost constant for these alloys).

To test whether the enhanced bcc orbital moment is an artifact of the VCA approximation for the disordered alloy, we have also performed calculations for the ordered alloy $\text{Co}_{0.5}\text{Ni}_{0.5}$ in the CsCl structure. The magnetization direction was as before in the z direction. The results from (SO) and (OP) calculations are shown in Table I together with the VCA results. The average spin and orbital moments are quite similar. In agreement with the results for the pure elements the spin and orbital moments are larger for the Co atom than for the Ni atom. However, there are deviations from the moments found in the pure elements, especially for the orbital moment. Consequently, the average orbital polarization for the ordered

TABLE I. Comparison between VCA and CsCl calculations for $\text{Co}_{0.5}\text{Ni}_{0.5}$. The spin and orbital moments are given in units of Bohr magnetons. The two upper rows refer to results from (SO) calculations and the two lower rows to (OP) calculations.

		CsCl			VCA (bcc)
		Co	Ni	Average	
(SO)	spin	1.63	0.63	1.13	1.11
	orbital	0.105	0.074	0.09	0.11
(OP)	spin	1.63	0.63	1.13	1.11
	orbital	0.240	0.075	0.16	0.17

TABLE II. Comparison between VCA and CsCl calculations for $\text{Fe}_{0.5}\text{Co}_{0.5}$. The spin and orbital moments are given in units of Bohr magnetons. The two upper rows refer to results from (SO) calculations and the two lower rows to (OP) calculations.

		CsCl			VCA (bcc)
		Fe	Co	Average	
(SO)	spin	2.69	1.71	2.20	2.18
	orbital	0.065	0.074	0.07	0.09
(OP)	spin	2.69	1.71	2.20	2.18
	orbital	0.092	0.106	0.10	0.13

compound exceeds the value obtained by linear interpolation between the two pure elements, and follows the VCA results. Notice also that the average orbital moment is enhanced in the (OP) calculation. From the results listed in Table I, we conclude that for the real systems there will be an enhanced orbital polarization for the alloy bcc phase. The possibility of observing this effect, of course, depends on whether these metastable systems can be grown; the current progress in epitaxial growth techniques seems very promising in this respect.

We also performed calculations for the ordered $\text{Fe}_{0.5}\text{Co}_{0.5}$ compound in the CsCl structure. In Table II the results are compared with the VCA results. Again the CsCl calculations give similar average spin and orbital moments to the VCA results. The relatively small differences between these two extreme cases, namely, a fully ordered and a completely disordered alloy, suggest that using VCA for the present alloys is a good approximation.

IV. CONCLUSION

The success of the VCA theory in explaining the experimental trends and even absolute values of the spin and

orbital moments of the Fe-Co-Ni alloys leads us to conclude that band-filling effects to a large extent explain the observed experimental data. The largest disagreement between experiment and theory is found for $\sim 50\text{--}75\%$ Co in Fe. The largest disagreement between experimental and calculated spin moments is also found for these alloys (Fig. 1), where our calculations overestimate the spin moment. Richter and Eschrig²⁰ calculated with CPA (coherent potential approximation) the same disagreement with experiment for the spin moment. This suggests that VCA is not responsible for this discrepancy. The corresponding orbital moments are overestimated as well and for that reason we performed calculations with the spin moment fixed to its experimental value, using the fixed-spin-moment method. The orbital moment was, however, found to be insensitive to small shifts in the spin moment and the disagreement for the orbital moment could therefore not be explained by the discrepancy in the spin moment. In the present paper, we have shown that the orbital moment for the stable crystal structure alloys contributes between $\sim 4\%$ and $\sim 13\%$ to the total moment and is therefore non-negligible. All three Hund's rules are needed to account for the size of the orbital moment. On the other hand, we find (not shown in the figures) that the spin moment is insensitive to the level of approximation (SP, SO, or OP). Finally, a strongly enhanced orbital moment is predicted for $x \sim 0.2\text{--}0.5$ for the hypothetical bcc $\text{Co}_{1-x}\text{Ni}_x$ alloys.

ACKNOWLEDGMENTS

P.S. is grateful to The Bank of Sweden Tercentenary Foundation and to the Göran Gustafsson Foundation for financial support. B.J. is grateful to The Swedish Natural Science Research Council for financial support. The support from the Nuclear Materials Division at Los Alamos is highly appreciated. Valuable discussions with B. R. Coles are also acknowledged.

- ¹J. F. Janak and A. R. Williams, *Phys. Rev. B* **14**, 4199 (1976).
²V. L. Moruzzi, J. F. Janak, and A. R. Williams, *Calculated Electronic Properties of Metals* (Pergamon, New York, 1978).
³O. K. Andersen, J. Madsen, U. K. Poulsen, O. Jepsen, and J. Kollar, *Physica* **86-88B**, 249 (1977).
⁴See also articles in *Ferromagnetic Materials*, edited by E. P. Wohlfarth and K. H. J. Bushow (Elsevier, Amsterdam, 1988).
⁵H. L. Skriver, *The LMTO Method* (Springer, Berlin, 1984).
⁶R. Feder, F. Rosicky, and B. Ackermann, *Z. Phys. B* **52**, 31 (1983); P. Strange, J. Staunton, and B. L. Gyorffy, *J. Phys. C* **17**, 3355 (1984); G. Schadler, P. Weinberger, A. M. Boring, and R. C. Albers, *Phys. Rev. B* **34**, 713 (1986); H. Ebert, P. Strange, and B. L. Gyorffy, *J. Phys. F* **18**, L135 (1988).
⁷O. K. Andersen, *Phys. Rev. B* **12**, 3060 (1975); M. S. S. Brooks and P. J. Kelly, *Phys. Rev. Lett.* **51**, 1708 (1983).
⁸O. Eriksson, B. Johansson, and M. S. S. Brooks, *J. Phys. Condens. Matter* **1**, 4005 (1989); O. Eriksson, M. S. S. Brooks, and B. Johansson, *Phys. Rev. B* **41**, 9087 (1990).
⁹O. Eriksson, B. Johansson, R. C. Albers, A. M. Boring, and M. S. S. Brooks, *Phys. Rev. B* **42**, 2707 (1990); O. Eriksson, L. Nordström, A. Pohl, L. Severin, A. M. Boring, and B.

- Johansson, *ibid.* **41**, 11 807 (1990).
¹⁰M. B. Stearns, in *Magnetic Properties of 3d, 4d and 5d Elements, Alloys and Compounds*, edited by K.-H. Hellwege and O. Madelung, Landolt-Börnstein, New Series, Vol. III/19a (Springer, Berlin, 1984); D. Bonnenberg, K. A. Hempel, and H. P. J. Wijn, *ibid.*
¹¹P. Soven, *Phys. Rev.* **156**, 809 (1967).
¹²J. Kübler, *J. Magn. Magn. Mater.* **15-18**, 859 (1980).
¹³See, for instance, J. M. Ziman, *Models of Disorder* (Cambridge University Press, Cambridge, England, 1979).
¹⁴U. von Barth and L. Hedin, *J. Phys. C* **5**, 1629 (1972).
¹⁵G. Racah, *Phys. Rev.* **62**, 438 (1942).
¹⁶E. C. Stoner, *Rep. Prog. Phys.* **11**, 43 (1943).
¹⁷V. L. Moruzzi, *Phys. Rev. Lett.* **57**, 2211 (1986).
¹⁸A. R. Williams, V. L. Moruzzi, J. Kübler, and K. Schwarz, *Bull. Am. Phys. Soc.* **29**, 278 (1984); K. Schwarz and P. Mohn, *J. Phys. F* **14**, L129 (1984).
¹⁹H. Ebert, R. Zeller, B. Drittler, and P. H. Dederichs, *J. Appl. Phys.* **67**, 4576 (1990).
²⁰R. Richter and H. Eschrig, *J. Phys. F* **18**, 1813 (1988).